

DEVELOPMENT OF A CORONARY FLOW MODEL FOR AORTIC VALVE TESTING

A Thesis
Presented to
The Academic Faculty

by
Eve George

In Partial Fulfillment
of the Requirements for the Degree
Biomedical Engineering in the
Coulter Department of Biomedical Engineering

Georgia Institute of Technology
May 2017

DEVELOPMENT OF A CORONARY FLOW MODEL FOR AORTIC VALVE TESTING

Approved by:

Dr. Ajit Yoganathan, Advisor
School of Biomedical Engineering
Georgia Institute of Technology

Dr. Sun Wei
School of Biomedical Engineering
Georgia Institute of Technology

Date Approved: May 1, 2017

ACKNOWLEDGEMENTS

I would like to thank Dr. Yoganathan and the entire Cardiovascular Fluid Mechanics Lab for supporting my research. I would especially like to thank my research mentors, Vrishank Raghav and Prem Midha, for their continued guidance and support. I would also like to acknowledge Beth Stayduhar who helped me immensely in completing this project.

TABLE OF CONTENTS

	Page
ACKNOWLEDGEMENTS	iv
LIST OF FIGURES	vi
SUMMARY	vii
<u>CHAPTER</u>	
1 Introduction	1-3
2 Methods	4-9
Georgia Tech Left Heart Simulator	4
Coronary Flow Model	5-6
Hemodynamics	7
Particle Image Velocimetry	8
Statistical Analysis	9
3 Results	10-14
Hemodynamics	10
Particle Image Velocimetry	11-14
4 Discussion	15-16
5 Limitations	17
6 Conclusion	17
REFERENCES	18-20

LIST OF FIGURES

Title	Page
Figure 1: Flow Loop Diagram	5
Figure 2: Aortic Valve Chamber	6
Figure 3: Proportional Pinch Valve and Stepper Drive	6
Figure 4: LabVIEW vi	7
Figure 5: Experimental Flow Profiles	10
Figure 6: PIV Comparisons	11-12
Figure 7: Peak Systole Timepoint Comparison	13
Figure 8: Valve Closure Timepoint Comparison	14
Figure 9: Early Diastole Comparison	14

SUMMARY

Transcatheter aortic valve replacement is a promising new technique to treat patients with severe aortic stenosis due to its minimally invasive approach. Unfortunately, higher levels of thrombosis from utilizing this device instead of a standard surgical aortic valve means further research is needed to understand the cause. In order to understand areas of flow stasis and accurately model local flow patterns, a coronary flow model was developed which produces more physiologically accurate flow conditions than aortic flow models without this feature. Two experiments were performed, with and without the coronary, and hemodynamic and particle image velocimetry (PIV) data were collected. The results showed differences in the magnitude and flow patterns between the two cases during systole. Relevant applications of this system include studying the effect of coronary flow on flow patterns within a transcatheter aortic valve in the context of valve thrombosis.

CHAPTER 1

INTRODUCTION

Approximately 1.5 million Americans suffer from aortic stenosis (AS), the narrowing of the aortic valve opening.¹ Over time, calcium (a mineral found in the blood), may accumulate on the aortic valve cusps. This process, known as calcification often results in the stiffening of the leaflets.² This stiffening prevents the aortic valve from fully opening, thereby increasing the resistance the left ventricle must overcome in order to eject blood into the aorta.² To make up for this loss, the ventricle compensates by pumping harder. In severe cases, aortic stenosis requires a valve replacement surgery.

For patients with severe symptomatic AS who are classified high surgical risk or inoperable, there is a new approach called transcatheter aortic valve replacement (TAVR).³ This procedure is performed percutaneously via catheter and the valve is deployed in a manner similar to a stent deployment. The valve is positioned within the native valve, pushing the calcified leaflets out of the way. This technique is very promising as it does not require open heart surgery, however further research needs to be conducted so that any complications and negative long term effects can be minimized.

One review of the most relevant complications associated with TAVR elucidates several issues related to the coronary arteries, which supply blood to the heart muscle.⁴ Malpositioning of the valve can lead to blocking of the coronary ostia. The correct anatomical location of valve deployment is within the aortic annulus so a deployment that is too deep (specific values vary based on patient anatomy) may block or alter flow patterns near the coronaries which are downstream of the annulus. Additionally, certain surgical techniques such as using a larger-diameter prosthesis may improve the

attachment between the prosthesis and the annulus thereby reducing the risk of paravalvular leak; however, this method would increase the risk of embolizing the debris from the calcified valve into the coronary arteries. Furthermore, recent studies which examine clinical data of TAVR patients have shown that the cases of valve thrombosis, the development of blood clots, are higher than expected.⁵⁻⁹ It is still unknown what leads to these higher levels of thrombosis, but it has been shown that hemodynamics play a key role in its progression.¹⁰⁻¹² With valve malpositioning being a known issue, this may result in abnormal flow patterns in and around the valve, thereby leading to stagnation of flow and ultimately a pro-thrombogenic environment.

In order to better understand the progression of thrombosis post-TAVR, researchers have developed several *in vitro* and computational models to simulate pulsatile blood flow through the aortic valve.¹³⁻¹⁵ Laadhari employs mathematical and computational modeling to study the incidence of blood stagnation after TAVR in the two-dimensional case.¹³ Vahidkhah performs an *in vitro* assessment of aortic valve hemodynamics along with computer simulations of the flow field.¹⁴ Ducci shows via an *in vitro* study that transcatheter aortic valves alter the physiological blood flow, and may lead to thromboembolic events.¹⁵ These studies, although thorough, do not incorporate the coronary arteries into their models. As a result, they do not capture the complete hemodynamic profile of the aortic sinus. Therefore, a model which incorporates the coronary arteries would aid in the process of understanding thrombosis development in TAVR patients.

Some previous studies have incorporated the coronary arteries into their models in an effort to achieve a more physiologically accurate model. Moore and Dasi constructed a

time-varying Windkessel chamber in order to model the effect of systolic coronary constriction.¹⁶ Querzoli uses a water-filled chamber to simulate the compression of the coronary by the cardiac muscle.¹⁷ Calderan et al. utilized a two-way stopcock valve controlled with a stepper motor via a LabView program.¹⁸ These studies have begun to show the effects of including the coronary arteries in aortic valve modeling however such models have yet to be applied to transcatheter aortic valves so. A more recent study does begin to quantify coronary velocity with a transcatheter aortic valve in place and compares this case to a non-coronary case. The study reveals that velocity through the sinus is reduced in the case without the coronary and that peak shear stress is higher along the aortic side of the coronary when compared to the non-coronary experiment.¹⁹ Further, more extensive research is still needed to fully understand the impact of TAVR on hemodynamics and what this means in clinical applications.

To better understand regions of flow stasis which may contribute to thrombosis development, a more physiologically accurate model is required to model local flow patterns through the aortic sinus. Therefore, the aim of this study is to create a physiologically relevant left heart simulator with coronary artery flow. A fully controllable and physiological coronary waveform is produced using a programmable variable pinch valve representing coronary resistance. A particle image velocimetry (PIV) experiment shows a difference between the model with and without coronary flow. This model can be used in future studies to understand blood flow patterns in the aorta and coronary with a transcatheter aortic valve in place.

CHAPTER 2

METHODS

Georgia Tech Left Heart Simulator

The Georgia Tech Left Heart Simulator (GTLHS) is a pulsatile flow loop that has been validated to mimic physiological hemodynamic conditions of the heart (Figure 1). Aortic valves to be tested can be mounted within the valve chamber which is idealized, rigid, and created to simulate the aortic root and proximal ascending aorta of a healthy adult. Physiologic aortic and ventricular pressures were attained by tuning the lumped resistance and compliance elements in the system which represent systemic vascular compliance and resistance. The bladder pump, which models the left ventricle, was controlled through a system of solenoid valves. The timing of the solenoid valves was controlled by a custom LabVIEW vi (National Instruments Corporation, Austin, TX). The GTLHS was tuned to a cardiac output of 5.0 L/min, aortic pressures of 120/80 mmHg, and a cardiac cycle length of 856 ms. Flow and pressure data was measured using an electromagnetic flow probe (Carolina Medical Electronics, East Bend, NC) and two pressure transducers (Validyne Engineering Corp, Northridge, CA). Data were acquired at a sampling frequency of 2000 Hz and averaged over 15 cardiac cycles.

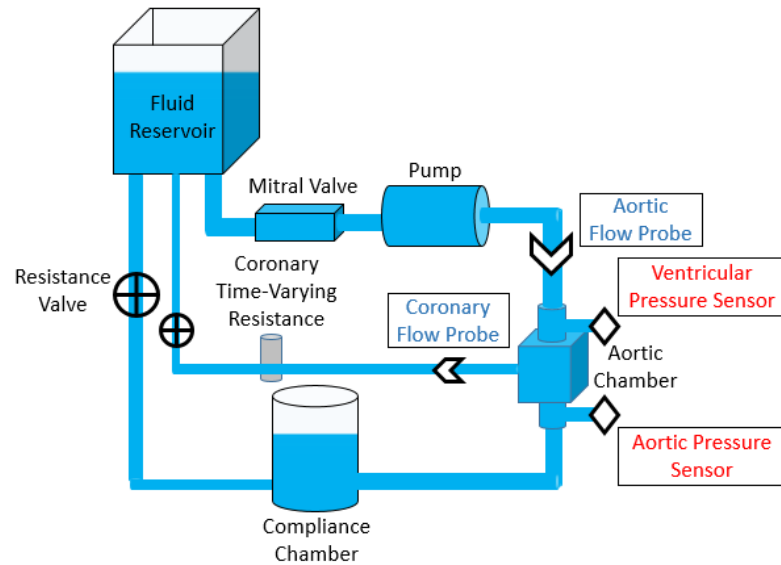


Figure 1. Flow Loop Diagram – Shows a schematic of the GTLHS with coronary addition.

Coronary Flow Model

In the aortic flow chamber described above, a 4 mm coronary ostium was added 17 mm above the aortic annulus. The coronary ostia location and size represents a patient average location based on previous studies^{.20-21} Figure 2 displays the model representation of the aortic sinus including a 27 mm Trifecta surgical aortic valve (St. Jude Medical, Saint Paul, Minnesota) and the coronary ostium. In order to mimic the coronary constriction that occurs from myocardial contraction, time-varying resistance was imposed on the coronary artery using a proportional pinch valve and stepper motor (ResolutionAir, Cincinnati, OH). The proportional pinch valve was wired to the stepper drive (Figure 3). The drive has two inputs (direction and step) which were wired to the analog output channels of a data acquisition system (cDAQ, National Instruments Corporation, Austin, TX). The stepper motor was connected to a 12-40V DC power source (BK Precision Corporation, Yorba Linda, CA). The cDAQ was connected to a

laptop which contained a custom LabVIEW code, which controls the oscillatory motion of the pinch valve. The frequency was set to 1.17 Hz to match the timing of the cardiac cycle. Coronary flow data was collected using an ultrasonic flow probe (Transonic Systems Inc., Ithaca, NY). Specific waveforms were produced in LabVIEW and used to control the stepper motor which controlled the direction and step of the pinch valve (Figure 4).

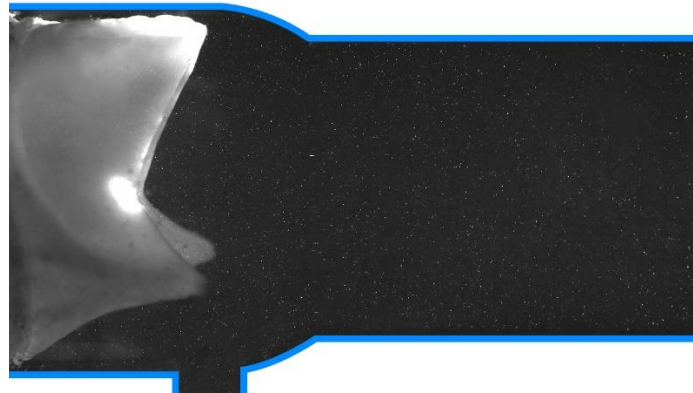


Figure 2. Aortic Valve Chamber - Aortic valve chamber with Trifecta surgical valve in place and coronary ostium.



Figure 3. Proportional Pinch Valve and Stepper Drive – (a) Proportional pinch valve used for the coronary experiments to mimic systolic constriction of the coronary. (b) Stepper

drive used to control proportional pinch valve (adapted from <http://www.resolutionair.com>).

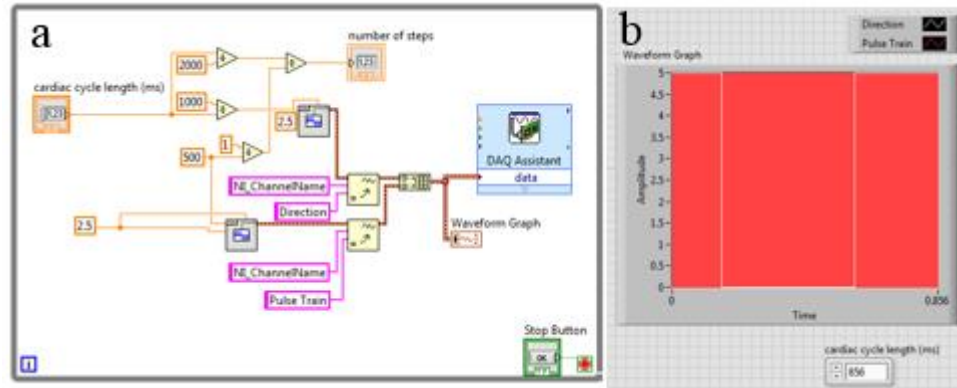


Figure 4. LabVIEW vi - (a) LabVIEW code used to send specific waveforms to the stepper motor and control the pinch valve. (b) Direction and pulse train waveforms produced by the LabVIEW code to control the pinch valve.

Hemodynamics

Experiments with and without a coronary artery were performed to collect and compare hemodynamic data of the two cases using a 27 mm Trifecta surgical aortic valve (St. Jude Medical, Saint Paul, Minnesota). Mean transvalvular pressure gradient, and effective orifice area were hemodynamic metrics calculated from the aortic pressure, ventricular pressure, and aortic flow data recorded from the validated LHS. Mean transvalvular pressure is the pressure gradient across the valve representing the difference in pressure between the left ventricle and aorta. Effective orifice area is the minimal cross-sectional area of flow downstream of the aortic valve. It is calculated using the following equation: $EOA = \frac{Q_{RMS}}{51.6 \sqrt{\Delta P / \rho}}$ where Q_{RMS} is the forward flow during the period of positive pressure differential, ΔP is the mean pressure gradient, and ρ is the test fluid

density. These metrics are used to assess the severity of aortic stenosis in patients.²²⁻²³

High pressures and low orifice areas indicate more severe cases of aortic stenosis.

Particle Image Velocimetry

Phase-locked PIV was used to investigate the effect of left coronary artery flow on the aortic sinus velocity field. PIV is a flow visualization technique which allows for the motion of neutrally buoyant particles to be quantified across a region of interest. The PIV experiments in this study yielded two-dimensional, two-component measurements. The working fluid used was a 3.5 cP saline-glycerine solution, 36% glycerin by volume in water, in order to match the kinematic viscosity of blood. The solution was seeded with fluorescent particles (PMMA with RhB dye, 1-20 μm , Dantec Dynamics; Denmark) which were illuminated using a laser sheet of 1 mm thickness generated from a Nd:YAG laser (New Wave laser, 532 nm, ESI Inc.; Portland OR). The particles were imaged with a CCD camera (LaVision, Germany, Imager ProX, 1600×1200 pixels). Two experiments were performed using a 27 mm Trifecta surgical aortic valve (St. Jude Medical, Saint Paul, Minnesota) with and without the coronary addition. The purpose of the experiments was to demonstrate any effect of the coronary on the flow field through the sinus. Data was collected at five different time points (0ms, 175ms, 300ms, 500ms, 700ms) throughout the cardiac cycle representing end diastole, peak systole, valve closure, peak coronary flow, and mid-diastole. Data at each timepoint was averaged over 200 cardiac cycles. PIV data processing was performed using DaVis 8.0 (LaVision GmbH, Goettingen, Germany).

Statistical Analysis

Two t-tests were performed in order to assess the significance of any differences between the hemodynamic data of the two experimental cases (with and without coronary). The mean transvalvular pressure gradient and the effective orifice area were the two metrics assessed. A p-value less than 0.05 was considered statistically significant.

CHAPTER 3

RESULTS

Hemodynamics

The experiment without the coronary was used as a baseline and produced a mean transvalvular pressure of 1.79 ± 0.194 mmHg while the coronary case produced a mean transvalvular pressure of 1.93 ± 0.264 mmHg ($p = 0.15$). Additionally, effective orifice area was 4.18 ± 0.18 cm² and 4.27 ± 0.24 cm² for the non-coronary and coronary cases, respectively ($p = 0.24$).

The aortic and coronary waveforms are shown in Figure 2. The first peak of the coronary flow rate waveform reaches a value of 0.3 L/min, reduces to 0.2 L/min, and then reaches a second peak value of 0.35 L/min. The curve then gradually declines to a value of 0 L/min. The average experimental coronary flow throughout the cardiac cycle is 157.87 mL/min.

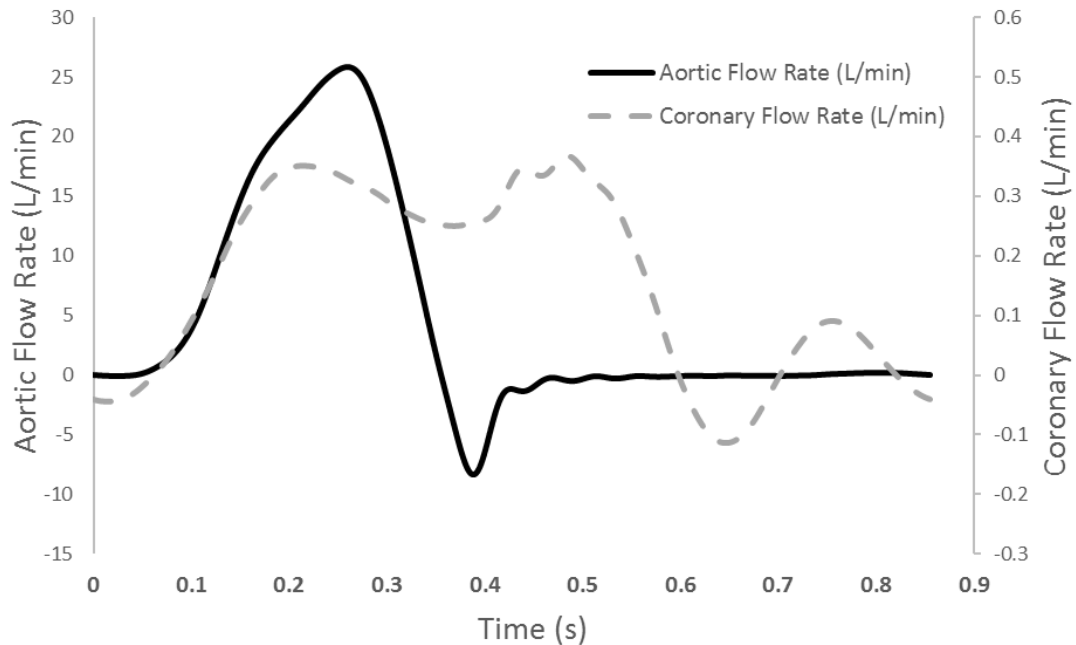
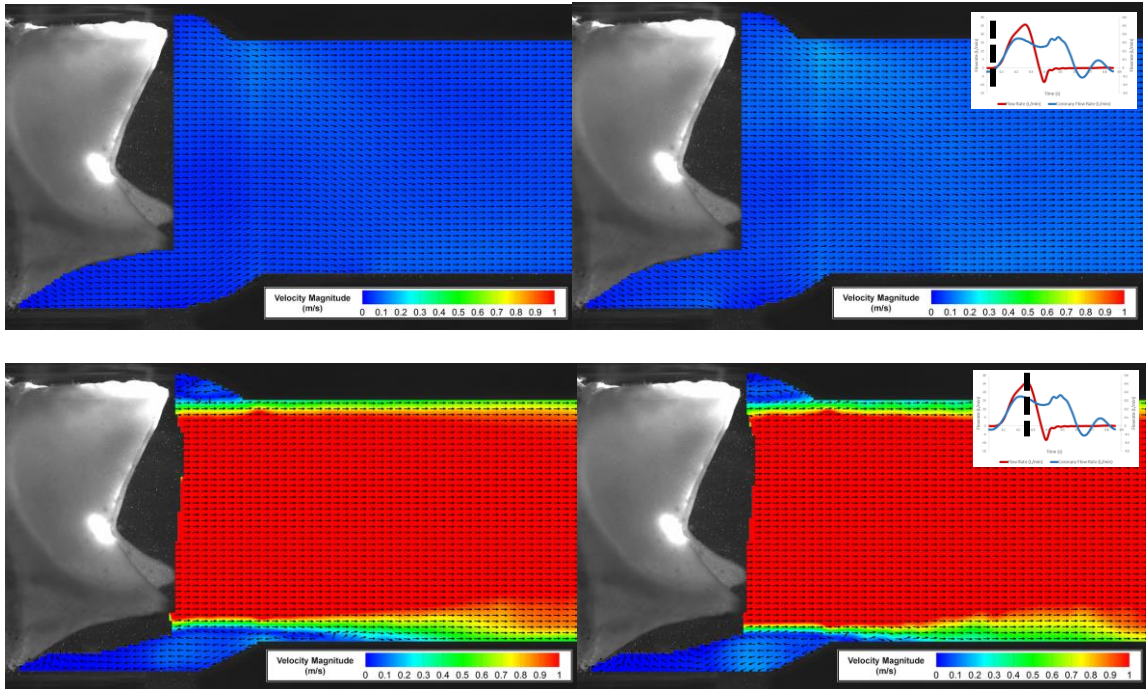


Figure 5. Experimental Flow Profiles – Aortic flow (solid line) and coronary flow (dashed line) averaged over 15 cardiac cycles.

Particle Image Velocimetry

Figures 6 and 7 compare flow through the aorta with and without the coronary addition at 5 different time points throughout the cardiac cycle. The color of the flow field indicates the magnitude and arrows indicate the direction of flow. At the end of diastole for both the coronary and non-coronary experiments, flow is quiescent with maximum velocities of 0.1 m/s or less. At peak systole, forward jet (velocities greater than 1m/s) encompasses almost the entire aorta in both cases. By valve closure, the magnitude of flow has decreased with both cases containing maximum velocity magnitudes of 0.5 m/s. During early diastole ($t=500$ ms) and mid-diastole ($t=700$ ms), the magnitude of flow is less than 0.1 m/s for both cases.



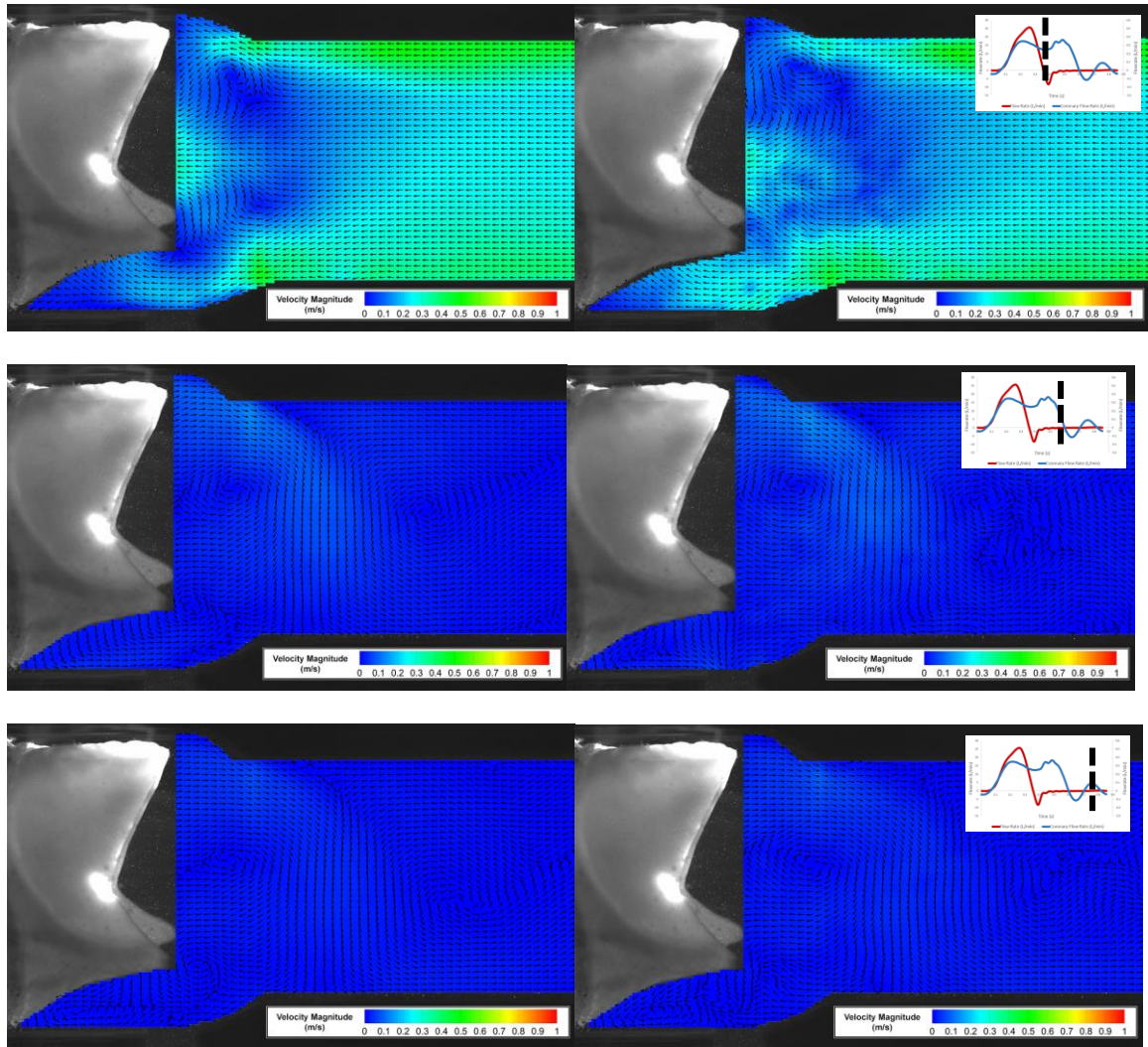


Figure 6. PIV Comparisons – Images show flow through the aorta at five different timepoints throughout the cardiac cycle (0ms, 175ms, 300ms, 500ms, 700ms) without (left column) and with (right column) the coronary model included. The color of the flow field indicates the magnitude, with red representing higher velocity flow (1 m/s) and blue representing lower velocity flow (0 m/s). Arrows point in the direction of flow.

At timepoints 175 ms and 300 ms, flow is directed toward the coronary ostium at slightly elevated velocities. At 175 ms, the velocity of flow without the coronary is nearly 0 m/s whereas this velocity is increased to 0.2 m/s once the coronary is incorporated

(Figure 8). This difference in velocity magnitude also occurs at 300 ms with a magnitude of 0.1 m/s for the non-coronary case and increasing to 0.3 m/s in the coronary case (Figure 9). Furthermore, at timepoint 500 ms, there are some key differences in the direction of the flow field of the coronary and non-coronary experiments. In the non-coronary experiment, there is an apparent vortex formed at the tip of the valve leaflet. On the other hand, the coronary experiment has flow pointing not toward the valve, but into the coronary ostium (Figure 9). Additionally, at the final timepoint, 700 ms (mid-diastole), the flow field is very quiescent in both cases since flow through the coronary is zero at this point in the cardiac cycle.

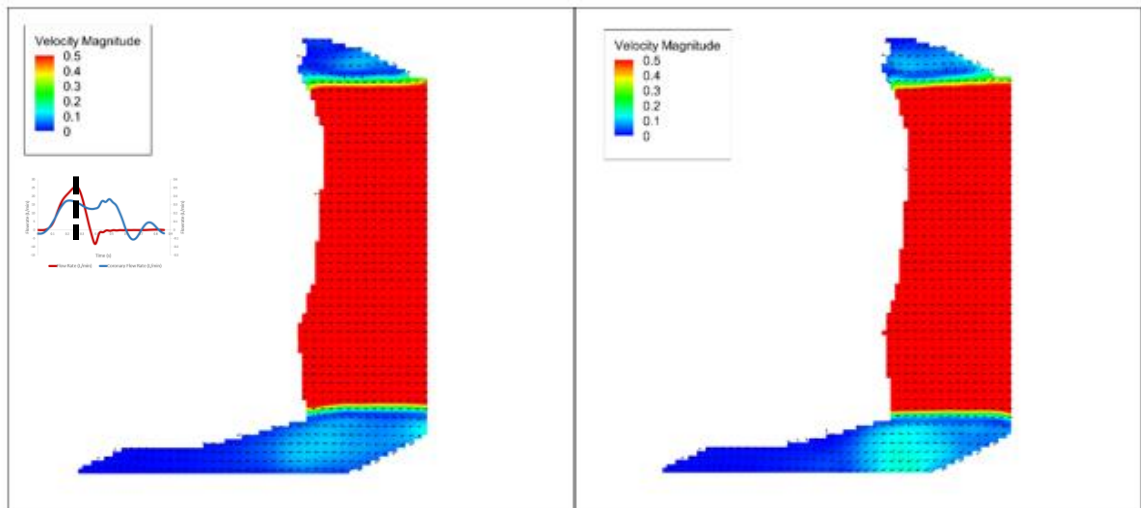


Figure 7. Peak Systole Comparison – Displays side-by-side comparison of non-coronary (left) and coronary (right) PIV experiments at 175 ms (peak systole).

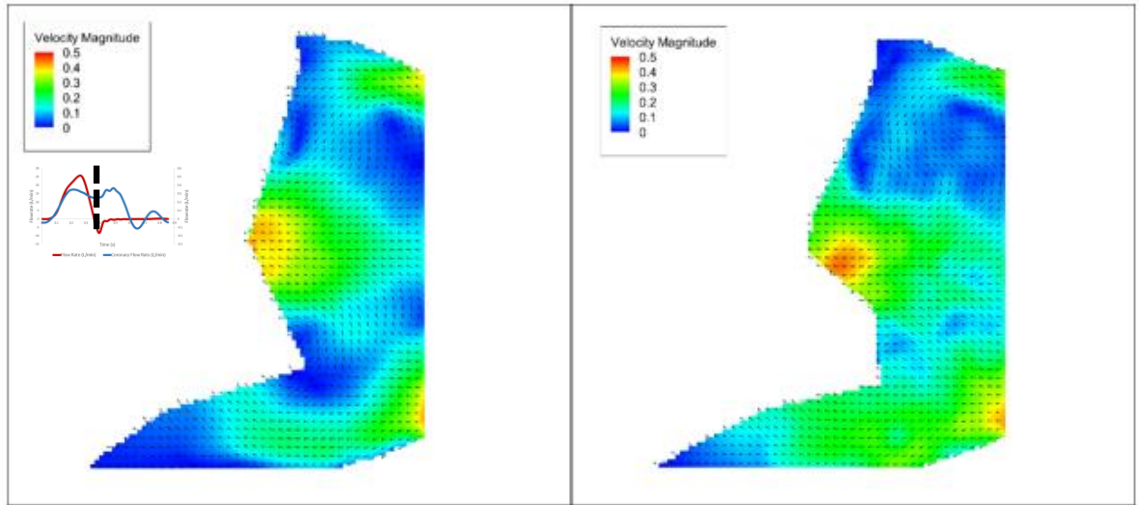


Figure 8. Valve Closure Comparison – Shows side-by-side comparison of non-coronary (left) and coronary (right) PIV experiments at 300 ms (valve closure).

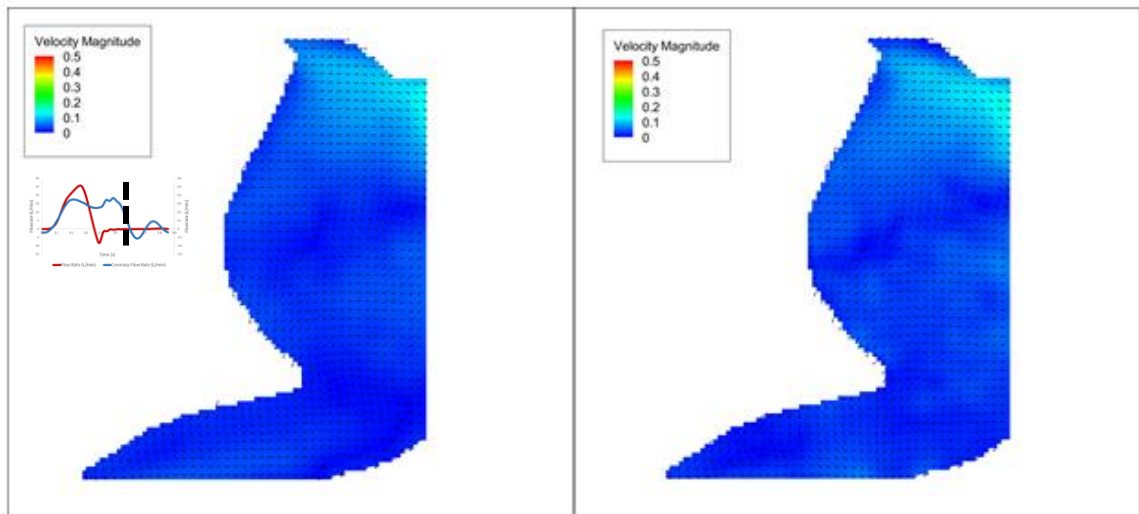


Figure 9. Early Diastole Comparison - Shows side-by-side comparison of non-coronary (left) and coronary (right) PIV experiments at 500 ms (early diastole).

CHAPTER 4

DISCUSSION

Hemodynamic metrics from each experimental condition were shown to not be statistically significantly different. This establishes that the system produces equivalent experimental environments for the non-coronary and coronary cases making PIV results directly comparable. Additionally, based on the hemodynamic results of the two experiments, the mean transvalvular pressure and the effective orifice area values are consistent with published values of the Trifecta valve.²⁴

A physiological coronary flow waveform is characterized by two peaks during the cardiac cycle. The initial peak, is the result of a rapid increase in the aortic pressure at the start of systole. Flow decreases when the myocardium is fully contracted, thereby constricting the coronary. The second peak arises during diastole as a result of myocardial relaxation which reduces resistance in the coronary. At the end of the waveform, flow steadily reduces to zero as aortic pressure decreases during diastole. Average physiological flow through the coronary during the cardiac cycle is 125 mL/min. Based on the results, the experimental system produced a waveform which is characterized by two peaks and thus matches the physiological expectations.

PIV experiments aided in elucidating the flow patterns and magnitudes in the sinus with and without the coronary. The addition of the coronary artery model resulted in changes in the flow field during peak and end systole in the region of interest, above the coronary. At peak systole, blood is being ejected from the left ventricle and in the region flowing into the coronary artery, the velocity magnitude is higher in the coronary case than the non-coronary case. This is logical because in the coronary case, blood can

flow continuously and unimpeded into the coronary and therefore produce higher magnitude flow in the region of interest. At valve closure (end systole), there is a similar region of higher magnitude flow near the coronary ostium in the coronary case than in the non-coronary case. The regions of higher magnitude flow in the coronary case correspond to the elevated coronary flow rates that occur during systole. The difference is further supported by directional arrows pointing into the location of the coronary ostium during systole for the coronary case but not the non-coronary case. During diastole, the flow fields between the two cases are comparable. This is logical because flow through the coronary is zero during diastole so it should not have an impact on the flow field through the sinus during these timepoints.

CHAPTER 5

LIMITATIONS

One limitation of this study stems from the timing characteristics of the timed coronary resistance component. The results showed a small peak in coronary flow after reaching zero however, physiologically, the flow should remain zero until systole. This slight error in the waveform arises from a hardware limitation meaning a pinch valve with a faster response time would allow for a more physiologically accurate time-varying resistance. Therefore, the proportional pinch valve timing system must be further optimized in order to produce a more physiologically accurate waveform. However, the results of this study demonstrate the feasibility of this system to generate physiologically relevant flow patterns in the aortic sinus adjacent to the coronary ostia.

CHAPTER 6

CONCLUSION

This study established a system which mimics coronary constriction during systole, thereby producing more physiologically accurate flow within the aortic sinus of the GTLHS. Finally, differences in flow magnitude and pattern were shown in experiments which compared cases with and without the addition of the coronary model. Further research on this system is needed to optimize the timing settings of the pinch valve system. Relevant applications of this system may be studying the effect of coronary flow on flow patterns within a transcatheter aortic valve in the context of valve thrombosis.

REFERENCES

1. Roberts WC, Ko JM. Frequency by decades of unicuspid, bicuspid, and tricuspid aortic valves in adults having isolated aortic valve replacement for aortic stenosis, with or without associated aortic regurgitation. *Circulation*. 111:920–925, 2005.
2. Baumgartner, H. Aortic stenosis: medical and surgical management. *Heart*, 91(11), 1483–1488, 2005.
3. Dasi, L. P., Hatoum, H., Kheradvar, A., Zareian, R., Alavi, S. H., Sun, W., Martin, C., Pham, T., Wang, Q., Midha, P., Raghav, V., Yoganathan, A. P. On the mechanics of transcatheter aortic valve replacement. *Ann Biomed Eng*, 1-22, 2016.
4. Neragi-Miandoab, S., & Michler, R. E. A Review of Most Relevant Complications of Transcatheter Aortic Valve Implantation. *ISRN Cardiology*, 2013.
5. Latib, A., Naganuma, T. Treatment and clinical outcomes of transcatheter heart valve thrombosis. *Circ Cardiovasc Interv*, 8, 2015.
6. De Marchena, E., Mesa, J., Pomenti, S., Marin y Kall, C., Marincic, X., Yahagi, K., Ladich, E., Kutz, R., Aga, Y., Ragosta, M., Chawla, A., Ring, M.E., Virmani, R. Thrombus Formation Following Transcatheter Aortic Valve Replacement. *JACC: Cardiovasc Interv*, 8(5), 728-739, 2015.
7. Córdoba-Soriano, J. G., Puri, R., Amat-Santos, I., Ribeiro, H. B., Abdul-Jawad Altisent, O., del Trigo, M., Rodés-Cabau, J. Valve Thrombosis Following Transcatheter Aortic Valve Implantation: A Systematic Review. *Revista Española de Cardiología (English Edition)*, 68(03), 198-204, 2015.
8. Leetma, T., Hansson, N. Early aortic transcatheter heart valve thrombosis diagnostic value of contrast-enhanced multidetector computed tomography. *Circ Cardiovasc Interv*, 8, 2015.
9. Mylotte, D., & Piazza, N. Transcatheter Aortic Valve Replacement Failure: Déjà vu ou Jamais vu? *Circ Cardiovasc Interv*, 8(4), 2015.
10. Weinberg, E. J., Mack, P. J., Schoen, F.J., Garcia-Cardena, G., Mofrad, M. R. K. Hemodynamic environments from opposing sides of human aortic valve leaflets evoke distinct endothelial phenotypes in vitro. *Cardiovasc. Eng*. 10:5–11, 2010.
11. Wootton, D.M., Ku, D.N. Fluid mechanics of vascular systems, diseases, and thrombosis. *Annual Review of Biomedical Engineering*. 1, 299-329, 1999.

12. Berger, S.A., Jou, L.D. Flows in stenotic vessels. *Annual Review of Fluid Mechanics*. 32, 347-382, 2000.
13. Laadhari, A. Warning about the risk of blood flow stagnation after transcatheter aortic valve implantation. *International Journal of Mathematical, Computational, Physical, Electrical and Computer Engineering*, 11(1) 33-37, 2017.
14. Vahidkhah K, Barakat M, Abbasi M, Javani S, Azadani PN, Tandar A, Dvir D, Azadani AN. Valve thrombosis following transcatheter aortic valve replacement: significance of blood stasis on the leaflets. *Eur J Cardio-Thoracic Surg*, 2017.
15. Ducci A, Pirisi F, Tzamtzis S, Burriesci G. Transcatheter aortic valves produce unphysiological flows which may contribute to thromboembolic events: An in-vitro study. *J Biomech*, 2016.
16. Moore, B. L., & Dasi, L. P. Coronary Flow Impacts Aortic Leaflet Mechanics and Aortic Sinus Hemodynamics. *Ann Biomed Eng*, 43(9), 2231-2241, 2015.
17. Querzoli, G., Fortini, S., Espa, S., & Melchionna, S. A laboratory model of the aortic root flow including the coronary arteries. *Experiments in Fluids*, 57(8), 2016.
18. Calderan, J., Mao, W., Sirois, E., & Sun, W. Development of an In Vitro Model to Characterize the Effects of Transcatheter Aortic Valve on Coronary Artery Flow. *Artificial Organs*, 2015.
19. Hatoum, H., Moore, B., Maureira, P., Dollery, J., Crestanello, J., & Dasi, L. P. Aortic Sinus Flow Stasis Likely in Valve-in-Valve Trans-Catheter Aortic Valve Implantation. *The Journal of Thoracic and Cardiovascular Surgery*, 2017.
20. Dodge, J. T., Brown, B. G., Bolson, E. L., & Dodge, H. T. Lumen diameter of normal human coronary arteries. Influence of age, sex, anatomic variation, and left ventricular hypertrophy or dilation. *Circulation*, 86(1), 232-246, 1992.
21. Knight, J., Kurtcuoglu, V., Muffly, K., Marshall, W., Jr., Stolzmann, P., Desbiolles, L., Alkadhi, H. Ex vivo and in vivo coronary ostial locations in humans. *Surg Radiol Anat*, 31(8), 597-604, 2009.
22. Nishimura, R. A., Otto, C. M., Bonow, R. O., Carabello, B. A., Erwin, J. P., Guyton, R. A., Thomas, J. D. 2014 AHA/ACC Guideline for the Management of Patients With Valvular Heart Disease. A Report of the American College of Cardiology/American Heart Association Task Force on Practice Guidelines. 2014.

23. Nishimura, R. A., Otto, C. M., Bonow, R. O., Carabello, B. A., Erwin, J. P., Fleisher, L. A., Thompson, A. 2017 AHA/ACC Focused Update of the 2014 AHA/ACC Guideline for the Management of Patients With Valvular Heart Disease: A Report of the American College of Cardiology/American Heart Association Task Force on Clinical Practice Guidelines. *Circulation*. 2017.
24. St. Jude Medical. The Trifecta Valve: In Vitro Hydrodynamic and Durability Comparisons of Aortic Bioprostheses, 2010.